High-rate viscoelastic shear model of porcine skin, lung and liver tissue

Joost Op ‘t Eynde, Christopher P. Eckersley, Cameron R. Bass

Abstract Computational models that evaluate high-rate loading scenarios to the thorax rely on material properties of the impacted soft tissues. The shear behaviour of these soft tissues, including viscoelastic stress relaxation, needs to be accounted for in an accurate model. Pure shear tests at high rate and high shear strain were performed on porcine dorsal skin, ventral skin, liver and lung tissue post-mortem. Synthetic gelatin was subjected to the same shear tests, to evaluate its validity as a tissue surrogate. Instantaneous elastic shear properties of the tissues were determined, and their stress relaxation over short (1 ms) and long (20 s) timescales. Dorsal skin tissue was found to have the highest shear stiffness, followed by ventral skin, liver and lung. Synthetic 20% gelatin approximates the instantaneous elastic shear properties of porcine dorsal skin but does not show the same viscoelastic relaxation behaviour. Synthetic 10% gelatin behaved similarly to 20% gelatin in stress relaxation, but with significantly reduced shear stiffness. Shear moduli of biological tissues increase with increased shear strain, suggesting a non-linear model is appropriate for computational purposes. A future determination of shear properties for human tissues will allow for a quantitative evaluation of using porcine tissue as a surrogate.

Keywords High-rate shear, Pig, Soft tissue, Synthetic gelatin, Viscoelasticity.

I. INTRODUCTION

Ballistic body armour provides protection to both civilian and military victims of high-velocity gunshot wounds to the chest and abdomen, reducing both mortality rates and injury severity [1]. By reducing the risk of bullet penetration and decreasing the total energy transferred to the body, the use of body armour by law enforcement officers more than triples the estimated likelihood of survival from gunshots to the torso [2]. When an incoming pistol or rifle round impacts body armour, the armour can stop the round by deforming, absorbing energy and momentum. Soft body armour readily deforms, while hard body armour deforms only after fracturing. The deformation at the backface of the body armour can impact underlying tissues, causing high-rate loading and injuries in the thorax. This is usually referred to as Behind Armour Blunt Trauma (BABT) [3].

To characterise the injuries caused by BABT, computational models with finite element (FE) analysis are often used. These models are an increasingly important research tool to simulate scenarios that are difficult and costly to test experimentally, and to understand local tissue behaviour. One example of models used is the Advanced Total Body Model (ATBM), used by the U.S. Department of Defense Non-Lethal Weapons Program [4]. For models to provide valid predictions for injuries and material behaviour, they rely on accurate mechanical properties of the biological tissues they represent. These tissues include not only the skeletal structure but also soft tissues such as the skin and internal organs. A 2012 report by the National Research Council stated that “The fidelity of anatomical, physical, and mathematical finite-element models simulating the human thorax, heart, lungs, liver, and kidneys, is limited” [5].

To accurately model soft tissues, their viscoelastic properties [6] must be accounted for. Mechanical properties of skin have been evaluated in literature using multiple different methods. Indentation testing has been used as a non-invasive in vivo method for human skin testing. In vivo indentation studies have shown viscoelastic behaviour of the skin at small amplitudes in quasi-static loading conditions [7-10] and up to sinusoidal loads of 60 Hz [11]. Historically, tension-compression testing of skin has been more common to determine material properties. This type of testing usually involved excising a skin sample to subject to loading conditions and has therefore often been conducted using animal specimens. Static and dynamic viscoelastic behaviour was observed in human and monkey scalp skin in tension and compression up to 40 Hz [12]. In wave transmission testing of

J. Op ‘t Eynde (e-mail: joost.opteynde@duke.edu; tel: +1-919-660-8272) and C.P. Eckersley are PhD students in Biomedical Engineering and C. R. Bass, PhD, is an Associate Research Professor in the Department of Biomedical Engineering at Duke University in Durham, NC, USA.

rabbit skin under uni-axial tension up to 1 kHz, a viscoelastic frequency dependence was observed [13]. In other studies, uni-axial and biaxial tensile testing on rabbit and human skin found rate-dependent stiffness and viscoelastic relaxation even at low rates [14-16]. To determine viscoelastic properties of skin at high frequencies, normal operating ultrasound transducers have been used [17-19]. While these experiments examine high-rate behaviour of the tissue, the strain levels are orders of magnitude smaller than the strain during BABT.

Because of the high water content in the liver and skin, these tissues are nearly incompressible (Poisson's ratio close to 0.5). They have a high bulk modulus and relatively low shear modulus. When impacted during BABT, the tissue under the impact will have predominantly local shear strains. To examine the shear response without confounding compressive stresses and the complex shear behavior of an indentation geometry, pure shear tests can be performed. However, pure shear loading has not often been a primary focus of soft tissue research. Some studies have investigated shear properties in skin using parallel plate rheometers [20-22], at low rates and/or low shear strain. Hollenstein *et al.* [23] conducted simple shear tests on large excised sections of porcine skin at a quasistatic rate. Gao *et al.* [24] performed shear, compression and tension tests on porcine liver tissue at low rates. To model impact scenarios such as BABT, material properties need to be tested at higher rates and large shear strain. In a more complex shear loading scenario, high rates have been achieved in soft tissues using a modified Kolsky bar (also known as a split-Hopkinson bar) [25], but no shear properties below 20% shear strain were reported.

Porcine skin has often been used as a surrogate for human skin since it is readily available, has similar mechanical properties [26,27], and there are histological and biochemical similarities between porcine and human skin [28]. In the current study, simple shear tests of post-mortem porcine skin, liver and lung tissue are performed, in a transverse orientation. The obtained shear properties can serve as a first approximation for human tissue properties.

Studies in the 1970s [29] relied on animal experiments and optical measurement of body armour backface deformation into a 20% gelatin block to determine a standard for evaluating body armour. After these initial studies, a pass/fail criterion of 44 mm backface deformation in Plastilina clay was developed to eliminate the need for difficult optical measurement techniques in the gelatin [30]. This criterion of 44 mm developed at the time is still in use today. More recent studies [31] have indicated that there is no correlation between this criterion and injuries seen in animal models, since clay is a poor surrogate for a thorax. There is a need for a different surrogate to evaluate body armour backface deformation. In the current study, we test the shear properties of 10% and 20% synthetic gelatin (Clear Ballistics, Greenville, SC, USA), to compare with the tested porcine tissues.

II. METHODS

Specimens

Porcine lung, liver, ventral skin covering the sternum, and dorsal skin from the thoracic region were obtained from 4–6-month-old Yorkshire pigs immediately post-mortem. The tissues were stored in saline at 4°C for maximally five days. Shortly before testing, porcine lung and liver tissue was cut into 10x10x10 mm cubes. Tissue specimens were cut from the ventral surface of the organs. Tissue specimens from the dorsal and ventral skin were cut in 10x10 mm squares, with the thickness being the local thickness of the skin (6–10 mm), including the adipose connective tissue underneath. Because samples were taken from skin areas where the directions of the Langer's lines are not clearly defined [32], their orientation was not considered as a variable. Synthetic 10% and 20% gelatin (Clear Ballistics, Greenville, SC, USA) was heated to 125°C, moulded into 10x10x10 mm cubes, and allowed to cool down to room temperature.

Shear Testing

Specimens were attached to two metal plates with a sandpaper surface in an ElectroForce testing machine (Bose Corporation, Framingham, Massachusetts, USA) (Fig. 1) using cyanoacrylate glue. Tests were conducted in a transverse orientation, with the surface of the organ spanning the gap between the two plates.

For each tissue type (dorsal skin, ventral skin, lung, liver, gelatin), five specimens were tested at room temperature (23.7°C +/- 1.9°C), and the specimen was kept hydrated with a saline spray.

A testing battery for each specimen consisted of a high-rate (~ 100 s^{-1}) ramp up to a shear strain level, held for 100 s to examine both the fast and slow viscoelastic relaxation behavior, ramp back to the original displacement, and held for 100 s. Strain levels of 10%, 15%, 30% and 40% shear strain were tested. Each strain level ramp was repeated three times to evaluate the tissue for possible local failure. A 10% shear strain test immediately followed by a 15% shear strain test was repeated three times, after which a 30% shear strain test

was repeated three times, and then a 40% shear strain test was repeated three times. The tests at higher shear strains were not performed in an alternating sequence so as not to lose testing data in case of tissue failure. In some cases, detachment of the tissue at higher strain levels occurred; the data for those strain levels were excluded from the results.

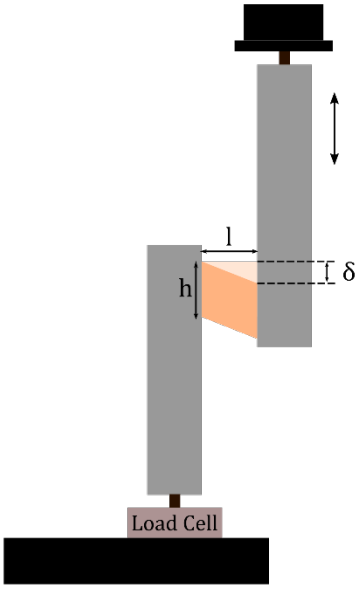

Fig. 1. Simple shear testing apparatus configuration. Specimen size is described by height (h), length (l), as indicated on the figure, and width (w) in the direction out of the figure plane. Displacement of the piston is represented with δ. Vertical force (F) is measured with a 10 N load cell.

Shear Strain and Stress

Displacement δ of the upper plate is measured as indicated in Fig. 1. Shear strain γ is then determined as:

$$\gamma = \frac{\delta}{l} \tag{1}$$

where l is the length of the specimen and distance between parallel plates, as shown in Fig. 1. Force F is measured by a 10 N load cell under the bottom plate. With h the height or thickness of the specimen, and w the width of the specimen along the plates (Fig. 1), the shear stress τ is calculated as:

$$\tau = \frac{F}{A} = \frac{F}{h \cdot w} \tag{2}$$

Force F and displacement δ were recorded at 20 kHz by a PicoScope 5444B oscilloscope (Pico Technology, Cambridgeshire, UK). During processing, the data traces were low pass filtered at 800 Hz.

Viscoelastic Models

To model shear stress (τ_M), quasilinear viscoelastic (QLV) behaviour was assumed, allowing for a separation of relaxation behaviour and nonlinear elastic behaviour, using a hereditary integral [6]:

$$\tau_M(\gamma, t) = \int_0^t R(t - t') \frac{d\tau_{el}(\gamma(t'))}{dt'} dt' \tag{3}$$

where R is the reduced relaxation function, t is time (in seconds) and t' is a dummy variable used for integration. This hereditary integral can be used to create a viscoelastic model given an arbitrary stress-strain history for the material. This method allows us to capture continuous relaxation even during the ramp loading. The relaxation function is a model for the behaviour of the material given a step strain, which is independent from the instantaneous elastic behavior of the material, i.e. elastic response without relaxation. The hereditary integral is a convolution of the relaxation function and instantaneous elastic function τ_{el}, which can be modeled linear as

$$\tau_{el} = G \cdot \gamma \tag{4}$$

with G the linear instantaneous elastic shear modulus; or modeled nonlinear as

$$\tau_{el} = A(e^{B\gamma} - 1) \tag{5}$$

resulting in exponential shear stress-strain behaviour with a toe region, as commonly seen in viscoelastic materials [6].

For the reduced relaxation function $R(t)$, a generalized Maxwell model is used, defined as:

$$R(t) = R_\infty + \sum_{i=1}^{n} R_i e^{-\beta_i t} \quad with \quad R_\infty + \sum_{i=1}^{n} R_i = 1 \tag{6}$$

where R_∞ is the steady-state relaxation coefficient, β_i is the inverse of a defined time constant for exponential relaxation, and R_i are the relaxation coefficients for each β_i term, expressed as a Prony series. After preliminary optimisation of the time constants using a subset of the data, the β_i are fixed to allow for comparisons to be made across specimens. For the current study, $n = 3$ was found to describe the viscoelastic relaxation to a reasonable accuracy without expanding the model too large. Chosen values for β_i were:

$$\beta_1 = 0.05\ s^{-1}\ \left(\frac{1}{20\ s}\right), \beta_2 = 1\ s^{-1}\ \left(\frac{1}{1\ s}\right), \text{and } \beta_3 = 100\ s^{-1}\ \left(\frac{1}{10\ ms}\right) \tag{7}$$

Model shear stress was calculated from the measured shear strain using the hereditary integral in Eq. 3, and the elastic and relaxation parameters were adjusted to fit the measured shear stress response from the tissue tests. Optimisation of instantaneous elastic parameters G or A and B, and viscoelastic relaxation parameters R_∞ and R_i was done using least squares fitting and a trust region optimisation algorithm in MATLAB® (MathWorks, Inc., Natick, MA, USA). Parameters were restricted to strictly positive values. Tissues were compared based on their instantaneous elastic parameters (cf. shear modulus), and viscoelastic relaxation coefficients R_∞ and R_i.

III. RESULTS

In observing the results of the ramp test repetitions, the second and third repetition of a ramp up to a certain strain level resulted in comparable stresses, but often significantly lower than the first ramp test. This might be occurring due to a softening effect from the first load to a new strain level, often referred to as the Mullins effect [33], or due to small local failures in the tissue or the tissue-adhesive interface. For material property analysis, the model output parameters from the second and the third test were averaged to give one result. Tissue failure was deemed to have occurred when the peak shear stress during a test was lower than the peak shear stress of that specimen in an earlier test at a lower shear strain level. Tests where tissue failure occurred were excluded from the analysis.

A comparison between the linear and the exponential form of the instantaneous elastic function showed that the tissues exhibited exponential stress-strain behaviour at higher strain levels (30% and 40%), while being mostly linear at lower strain levels (10% and 15%). An example of the exponential instantaneous elastic functions is shown in Fig. 2. For these dorsal skin models, the exponential form of the instantaneous elastic function improved the model fit over the linear form, reducing the sum of the squared error by 8.6% on average. This exponential elastic behaviour is indicative of a toe region, as commonly seen in biological materials. However, since both constants A and B can be changed to account for the elastic behaviour, it is difficult to compare shear moduli between specimens, except for a direct comparison of the stress-strain curves. Therefore, it was decided to use the linear form of the instantaneous elastic function to allow for comparisons between specimens.

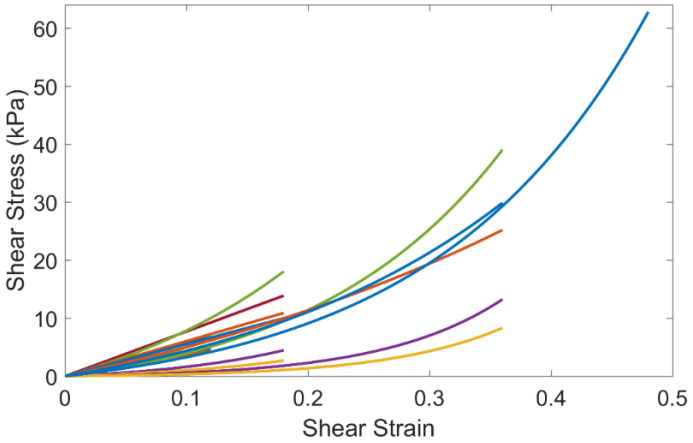

Fig. 2. Exponential models of instantaneous elastic shear stress functions for dorsal porcine skin samples. The stress-strain curve is linear at lower strain levels (10% and 15% shear strain), but shows an increase in stiffness at higher strains. Different specimens are indicated by the different colours on the graph.

The instantaneous elastic shear modulus values from the optimisation of the viscoelastic model can be found in Table I. As discussed earlier and seen in Fig. 2, there is an increase in shear modulus as the shear strain level increases. To compare the viscoelastic relaxation between specimens, the results of the reduced relaxation function optimisation for the 30% strain tests are compared. These results can be found in Table II. In biological tissues (skin, liver, lungs), more fast relaxation behaviour occurs than in the synthetic gelatin, as seen by the value of R_3. There is also overall less relaxation in the gelatin, even after 100 s, resulting in a larger steady state coefficient R_∞. A visual comparison of the long-term and short-term relaxation of dorsal skin and 10% gelatin can be found in Fig. 3–6. Example of relaxation in ventral skin and liver is shown in Fig. 7 and Fig. 8. In these figures, the measured shear strain (blue) and shear stress (orange) from the tissue tests is shown, together with the viscoelastic model fit shear stress (green) calculated based on the measured shear strain with parameters optimized to fit the measured shear stress.

TABLE I
SHEAR MODULUS G IN KPA (SD)

SPECIMEN TYPE	SHEAR STRAIN LEVEL			
	10%	15%	30%	40%
Dorsal Skin	34.0 (19.1)	53.8 (28.4)	57.1 (28.9)	66.7 (34.0)
Ventral Skin	14.0 (5.9)	17.8 (6.5)	16.9 (5.6)	17.6 (5.7)
Liver	4.0 (1.5)	7.8 (2.7)	10.8 (5.2)	11.0 (6.0)
Lung	4.5 (3.3)	2.6 (1.71)	3.5 (1.9)	4.0 (1.5)
10% Gelatin	38.0 (5.5)	33.7 (6.3)	32.5 (6.3)	38.3 (0.4)
20% Gelatin	/	64.5 (6.3)	57.3 (9.1)	57.5 (8.6)

TABLE II
VISCOELASTIC RELAXATION COEFFICIENTS (SD) FOR 30% SHEAR TEST

Specimen Type	Relaxation Coefficients (time constant)			
	R_∞	R_1 (20 s)	R_2 (1 s)	R_3 (10 ms)
Dorsal Skin	0.382 (0.192)	0.045 (0.009)	0.048 (0.022)	0.525 (0.218)
Ventral Skin	0.303 (0.096)	0.042 (0.012)	0.046 (0.016)	0.609 (0.609)
Liver	0.231 (0.054)	0.049 (0.007)	0.017 (0.014)	0.704 (0.064)
Lung	0.285 (0.147)	0.039 (0.042)	0.013 (0.025)	0.664 (0.139)
10% Gelatin	0.602 (0.065)	0.121 (0.012)	0.099 (0.019)	0.178 (0.069)
20% Gelatin	0.644 (0.038)	0.095 (0.009)	0.098 (0.016)	0.163 (0.038)

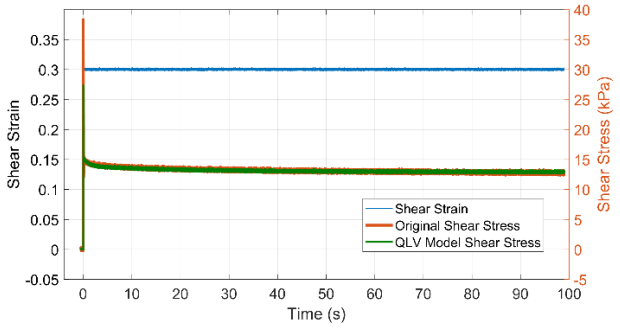

Fig. 3. Dorsal skin 30% shear test measurements. The stress calculated by the viscoelastic model is shown with the measured shear stress and strain.

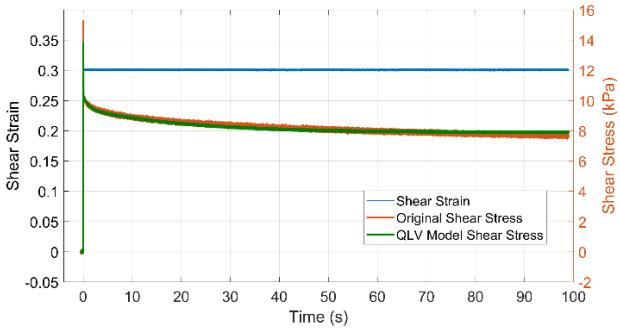

Fig. 4. 10% Gelatin 30% shear test measurements. The stress calculated by the viscoelastic model is shown with the measured shear stress and strain.

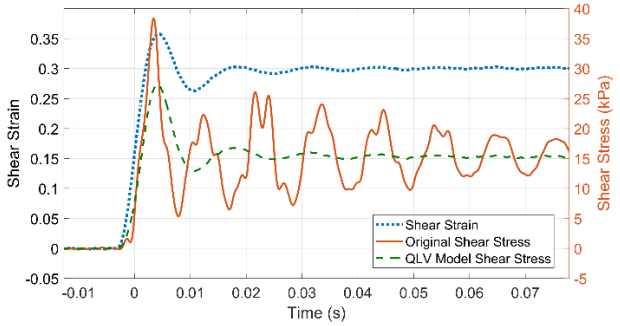

Fig. 5. Same dorsal skin test shown in Fig. 3, showing the ramp loading and fast relaxation behaviour. Clear oscillatory behaviour is seen in the shear stress.

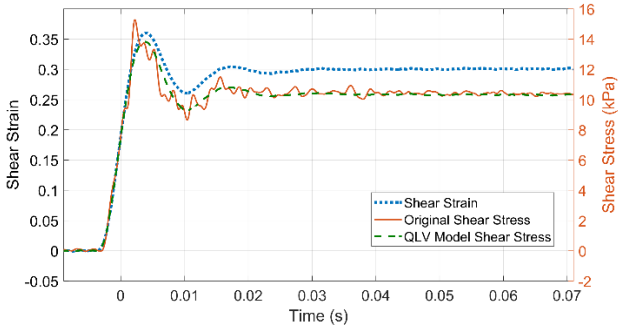

Fig. 6. Same 10% gelatin test shown in Fig. 4, showing the ramp loading and fast relaxation behaviour. Oscillatory behaviour is much less pronounced.

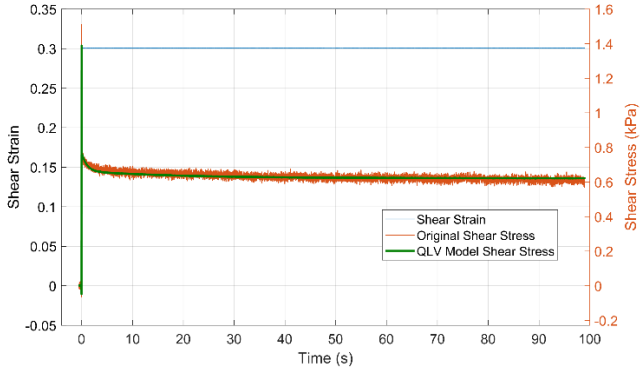

Fig. 7. Ventral skin 30% shear test measurements. The stress calculated by the viscoelastic model is shown with the measured shear stress and strain.

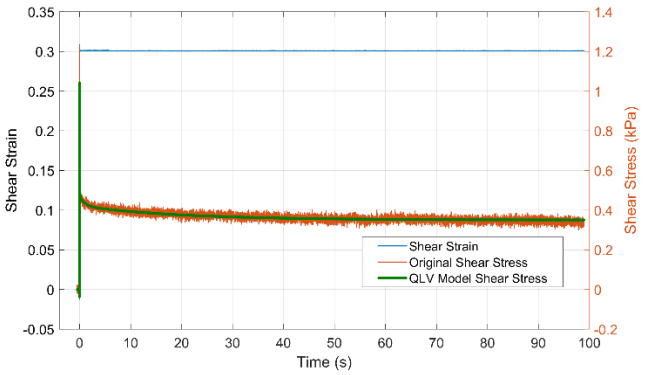

Fig. 8. Liver 30% shear test measurements. The stress calculated by the viscoelastic model is shown with the measured shear stress and strain.

In the biological tissue tests, e.g. Fig. 5, rapid oscillation of the stress at a frequency of approximately 100 Hz was observed immediately following the ramp. This behaviour can be an indication of inertial effects, caused by undamped deceleration of the specimen mass due to the sudden stop of the upper plate. In the gelatin tests, e.g. Fig. 6, this oscillatory behaviour is much less pronounced, potentially due to increased damping in the gelatin. The oscillatory behaviour dissipates after 10–15 ms. Because of these inertial effects, which are not included in the viscoelastic model, there is an overshoot of the peak shear stress, resulting in an underprediction of the peak stress by the model.

IV. Discussion

Linear and quasilinear viscoelastic models were developed and applied to high-rate, high amplitude pure shear tests on porcine biological tissues, including skin, liver and lung, and on synthetic gelatin. Good fit was achieved on the long-term relaxation of the models (Fig. 3–4, 7–8) and on the short-term relaxation, with the exception of inertial oscillations (Fig. 5). These models allow us to evaluate the shear strength of these materials at different strain levels, and to examine their temporal behaviour under a shear load. Tissues were tested at high rates, up

to 100 s^{-1}. While only a single loading strain curve was tested for each shear level, the use of a hereditary integral (Eq. 3) to model shear stress for the entire strain history incorporates loading behavior at all rates during the ramp, going up to maximum rate initially and slowing down near the final level.

Shear moduli (Table I) increase at higher strain levels, suggesting non-linear elastic behaviour. While linear shear was assumed in this study to compare tissues, computational models for biological tissues at high shear strain should include non-linear behaviour describing the toe region. The dorsal skin had the highest shear strength of the biological tissues, followed by the ventral skin and then the liver and lung. The 20% synthetic gelatin was comparable to the dorsal skin in shear strength. The 10% ballistics gelatin had shear moduli a little over half the values seen in the 20% gelatin and dorsal skin, but this was still significantly higher than the other tested tissues. The reported values exceed those reported in literature for low-rate loading [22,34], but fall below shear moduli reported in split-Hopkinson bar experiments [25]. Based on shear strength, 20% synthetic gelatin appears to be an appropriate surrogate for porcine dorsal skin.

When considering the viscoelastic relaxation however, synthetic gelatin does not behave in a similar manner to biological tissues (Table II). While all tested biological tissues have relatively similar relaxation coefficients, both 10% gelatin and 20% gelatin have reduced fast relaxation behaviour on the timescale of 10 ms (R_3). This initial period is when most of the viscoelastic relaxation occurs in biological tissues. Instead, gelatin has increased relaxation over longer timescales, 1 s (R_2) and 20 s (R_3), and a higher proportion of stress retained after 100 s (R_∞). Among the biological tissues, liver and lung tissue have more fast relaxation behaviour than ventral skin and even more so compared to dorsal skin.

Testing at room temperature is one of the limitations of the current study, since it has been shown that material properties of biological materials can depend on temperature [35]. Follow-up studies to the current one will include testing inside a temperature-controlled chamber. Additional variables will include the storage of the tissue specimen before testing, evaluating the validity of testing frozen and thawed biological tissues, and a parallel orientation for tissue shear testing, with the tissue surface parallel to the metal plates. Future studies for determination of the shear properties for human tissues will allow for a quantitative evaluation of using porcine tissue or synthetic gelatin as a surrogate.

V. CONCLUSIONS

Viscoelastic shear behaviour of porcine skin, lung and liver tissue can be accurately described by a quasilinear viscoelastic model with Prony series relaxation behaviour. Porcine dorsal skin has a comparable shear modulus to synthetic 20% gelatin, but the relaxation behaviour of synthetic gelatin is different from biological tissues. Shear moduli of biological tissues increase with increased shear strain, suggesting non-linear behaviour. The obtained shear properties can serve as a first approximation for shear properties of human tissues in computational models for high-rate impact scenarios.

VI. ACKNOWLEDGEMENTS

The authors gratefully acknowledge the funding and collaboration from MTEC-18-04-I-PREDICT-07, Incapacitation Prediction for Readiness in Expeditionary Domains, an Integrated Computational Tool (I-PREDICT) Thorax Model Prototype.

VII. REFERENCES

[1] Peleg K, Rivkind A, Aharonson-Daniel L, and Israeli Trauma Group. Does body armor protect from firearm injuries? *Journal of the American College of Surgeons*, 2006, 202(4):p.643–648.

[2] LaTourrette T. The life-saving effectiveness of body armor for police officers. *Journal of occupational and environmental hygiene*, 2010, 7(10):p.557–562.

[3] Bass CR, Salzar RS, et al. Injury risk in behind armor blunt thoracic trauma. *International journal of occupational safety and ergonomics*, 2006, 12(4):p.429–442.

[4] Shen W, Niu E, Webber C, Huang J, and Bykanova L. Advanced Total Body Model (ABTM) Analyst's Guide For Model Verification and Validation: San Diego, CA, USA, 2012.

[5] National Research Council. Testing of body armor materials: Phase III. National Academies Press: Washinton, DC, USA, 2012.

[6] Fung YC. Biomechanics: mechanical properties of living tissues. *Springer Science & Business Media*, New York City, USA, 2013.
[7] Bader D and Bowker P. Mechanical characteristics of skin and underlying tissues in vivo. *Biomaterials*, 1983, 4(4):p.305–308.
[8] Delalleau A, Josse G, Lagarde J-M, Zahouani H, and Bergheau J-M. Characterization of the mechanical properties of skin by inverse analysis combined with the indentation test. *Journal of biomechanics*, 2006, 39(9):p.1603–1610.
[9] Pailler-Mattei C, Bec S, and Zahouani H. In vivo measurements of the elastic mechanical properties of human skin by indentation tests. *Medical engineering & physics*, 2008, 30(5):p.599–606.
[10] Zahouani H, Pailler-Mattei C, et al. Characterization of the mechanical properties of a dermal equivalent compared with human skin in vivo by indentation and static friction tests. *Skin research and technology*, 2009, 15(1):p.68–76.
[11] Boyer G, Laquieze L, Le Bot A, Laquieze S, and Zahouani H. Dynamic indentation on human skin in vivo: ageing effects. *Skin Research and Technology*, 2009, 15(1):p.55–67.
[12] Galford JE and McElhaney JH. A viscoelastic study of scalp, brain, and dura. *Journal of biomechanics*, 1970, 3(2):p.211–221.
[13] Pereira J, Mansour J, and Davis B. Dynamic measurement of the viscoelastic properties of skin. *Journal of Biomechanics*, 1991, 24(2):p.157–162.
[14] Lanir Y and Fung Y. Two-dimensional mechanical properties of rabbit skin—II. Experimental results. *Journal of biomechanics*, 1974, 7(2):p.171–182.
[15] Sugihara T, Ohura T, Homma K, and Igawa H. The extensibility in human skin: variation according to age and site. *British journal of plastic surgery*, 1991, 44(6):p.418–422.
[16] Reihsner R, Balogh B, and Menzel E. Two-dimensional elastic properties of human skin in terms of an incremental model at the in vivo configuration. *Medical engineering & physics*, 1995, 17(4):p.304–313.
[17] Moran C, Bush N, and Bamber J. Ultrasonic propagation properties of excised human skin. *Ultrasound in medicine & biology*, 1995, 21(9):p.1177–1190.
[18] Diridollou S, Berson M, et al. An in vivo method for measuring the mechanical properties of the skin using ultrasound. *Ultrasound in medicine & biology*, 1998, 24(2):p.215–224.
[19] Pan L, Zan L, and Foster FS. Ultrasonic and viscoelastic properties of skin under transverse mechanical stress in vitro. *Ultrasound in medicine & biology*, 1998, 24(7):p.995–1007.
[20] Holt B, Tripathi A, and Morgan J. Viscoelastic response of human skin to low magnitude physiologically relevant shear. *Journal of biomechanics*, 2008, 41(12):p.2689–2695.
[21] Geerligs M, Oomens C, Ackermans P, Baaijens F, and Peters G. Linear shear response of the upper skin layers. *Biorheology*, 2011, 48(3-4):p.229–245.
[22] Lamers E, Van Kempen T, Baaijens F, Peters G, and Oomens C. Large amplitude oscillatory shear properties of human skin. *Journal of the mechanical behavior of biomedical materials*, 2013, 28:p.462–470.
[23] Hollenstein M, Ehret AE, Itskov M, and Mazza E. A novel experimental procedure based on pure shear testing of dermatome-cut samples applied to porcine skin. *Biomechanics and Modeling in Mechanobiology*, 2011, 10(5):p.651–661.
[24] Gao Z, Lister K, and Desai JP. Constitutive modeling of liver tissue: experiment and theory. *Annals of biomedical engineering*, 2010, 38(2):p.505–516.
[25] Saraf H, Ramesh K, Lennon A, Merkle A, and Roberts J. Mechanical properties of soft human tissues under dynamic loading. *Journal of biomechanics*, 2007, 40(9):p.1960–1967.
[26] Edwards C and Marks R. Evaluation of biomechanical properties of human skin. *Clinics in dermatology*, 1995, 13(4):p.375–380.
[27] Shergold OA, Fleck NA, and Radford D. The uniaxial stress versus strain response of pig skin and silicone rubber at low and high strain rates. *International Journal of Impact Engineering*, 2006, 32(9):p.1384–1402.
[28] Vardaxis N, Brans T, Boon M, Kreis R, and Marres L. Confocal laser scanning microscopy of porcine skin: implications for human wound healing studies. *The Journal of Anatomy*, 1997, 190(4):p.601–611.
[29] Goldfarb MA, Ciurej TF, Weinstein MA, and Metker LW. A method for soft body armor evaluation: medical assessment. National Technical Information Service: Springfield, VA, USA, 1975.
[30] Prather RN, Swann CL, and Hawkins CE. Backface Signatures of Soft Body Armors and the Associated Trauma Effects. Chemical Systems Laboratory: Aberdeen Proving Ground, MD, USA, 1977.
[31] Hanlon E and Gillich P. Origin of the 44-mm behind-armor blunt trauma standard. *Military medicine*, 2012, 177(3):p.333–339.

[32] Chu H, Son D, Kwon S, Kim J, and Han K. Characteristics of Wound Contraction according to the Shape and Antomical Regions of the Wound in Porcine Model. *Journal of the Korean Society of Plastic and Reconstructive Surgeons*, 2011, 38(5):p.576–584.
[33] Mullins L. Softening of rubber by deformation. *Rubber chemistry and technology*, 1969, 42(1):p.339–362.
[34] Liu Z and Bilston LE. Large deformation shear properties of liver tissue. *Biorheology*, 2002, 39(6):p.735–742.
[35] Bass CR, Planchak CJ, et al. The temperature-dependent viscoelasticity of porcine lumbar spine ligaments. *Spine*, 2007, 32(16):p.E436–E442.